Inorganic Chemistry

Article

pubs.acs.org/IC

Investigating the Electronic Structure of the Atox1 Copper(I) Transfer Mechanism with Density Functional Theory

Amanda L. Pitts and Michael B. Hall*

Department of Chemistry, Texas A&M University, College Station, Texas 77843-3255, United States

Supporting Information

ABSTRACT: To maintain correct copper homeostasis, the body relies on ion binding metallochaperones, cuprophilic ligands, and proteins to move copper around as a complexed metal. The most common binding site for Cu(I) proteins is the CX_1X_2C motif, where X_1 and X_2 are nonconserved residues. Although this binding site motif is well established, the mechanistic and electronic details for the transfer of Cu(I) between two binding sites have not been fully established, in particular, whether the transfer is dissociative or associative or if the electron-rich Cu(I)−Cys interactions influence the transfer. In this work, we investigated the electronic structure of the Cu(I)−S interactions during the copper transfer between Atox1 and a metal binding domain on the ATP7A or ATP7B protein. Initially, three Cu(I) methylthiolate complexes, $[Cu(SCH_3)_2]^{-1}$, $[Cu(SCH_3)_3]^{-2}$, $[Cu(SCH_3)_4]^{-3}$, were investigated with density functional theory (DFT) to fully elucidate the electronic structure and bonding between Cu(I) and thiolate species. The two-coordinate, linear species with a C−S−S−C dihedral angle of ∼90° is the lowest energy conformation because the filled π antibonding orbitals are stabilized in this geometry. The importance of π-overlap is also seen with the trigonal planar, three-coordinate Cu(I) complex, which is similarly stabilized. A corresponding four-coordinate species could not be consistently optimized, so it was concluded that tetrahedral coordination was not likely to be stable. The transfer of Cu(I) from the Atox1 metallochaperone to a metal binding domain of the ATP7A or ATP7B protein was then modeled by using the CGGC Atox1 binding site for the donor model and the dithiotreitol ligand (DTT) for the acceptor model. The two- and three-coordinate intermediates calculated along the five-step transfer mechanism converged to near optimal Cu−S π-overlap for the respective geometries, which demonstrates that the electronic structure in this electron-rich environment influences the intermediate's geometries in the transfer mechanism.

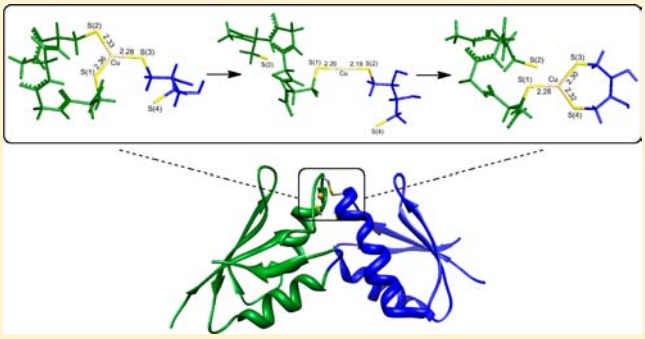

INTRODUCTION

Although copper, the third most abundant metal in the human body, is essential for proper function,[1] it is hazardous as an uncomplexed ion. Free copper ions can form radicals and reactive oxygen species (ROS) that are highly destructive and potentially fatal.[2] Understanding how the body maintains proper copper homeostasis is important in preventing or curing diseases associated with a build up or lack of copper. Several diseases known to be caused by an improper Cu(I) balance are Menkes disease,[1] familial amyotrophic lateral sclerosis,[3] and Wilson's disease.[4] Although these diseases are genetic and cannot be cured, they can be treated, but improving treatments depends on acquiring a deeper understanding of copper transfer inside the cell.[4] In addition, a build up of copper ions has also been linked to Alzheimer's[5] and prion[6] diseases. To maintain homeostasis, the body relies on ion binding metallochaperones, proteins, and other cuprophilic ligands to move Cu(I) around as a complexed metal. The proteins that bind Cu(I) are highly specific, and most have a conserved, CX_1X_2C, binding site motif, where X is a nonconserved amino acid that is not directly involved in the binding of Cu(I).[7]

There are several regulatory pathways for copper inside the cell, and each starts with the uptake of Cu(I) through a Ctr permease. These high-affinity copper transporters have methionine and cysteine binding sites that coordinate copper as it enters the cell.[8] Once in the cytoplasm there are three main destinations for a copper ion, the CcO enzyme in the mitochondria, the copper/zinc superoxide dismutase 1 (SOD1), or the ATPase proteins in the Golgi apparatus, Scheme 1. The ions are transferred to these destinations via metallochaperones that are specific to each path. The Cox17 metallochaperone initiates the Cu(I) delivery to the CcO enzyme,[9] and SOD1 primarily accepts Cu(I) from the CCS metallochaperone in the cytoplasm where it is used to protect the cell against ROS.[7,10] The Atox1 metallochaperone carries Cu(I) to the Golgi apparatus where it is then transferred to a metal binding domain of ATP7A or ATP7B. These ATPase proteins have four regions, the N-terminal, the transmembrane region, the ATP-binding region, and the phosphatase region. The N-terminal region is separated into six independently

Received: May 3, 2013
Published: August 26, 2013

   dx.doi.org/10.1021/ic401106z | Inorg. Chem. 2013, 52, 10387−10393

Scheme 1. The Three Main Cu(I) Pathways Inside the Human Cell with a Metallochaperone Specific to Each Destination[a]

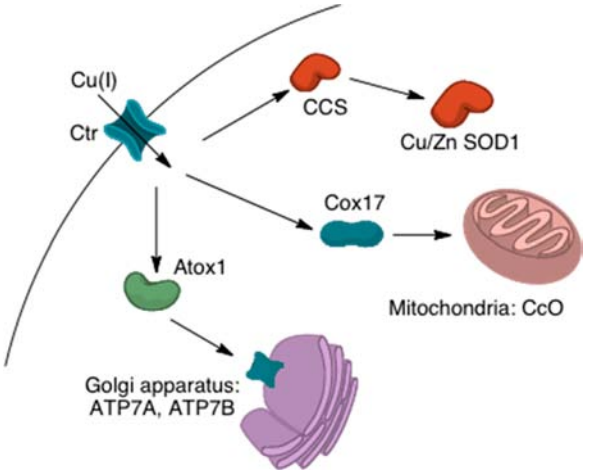

[a]Copper is transferred from the chaperones to the acceptor protein or enzyme depending on the path.

folded, 70-residue long domains. Inside each of the six domains, referred to herein as a metal binding domain (MBD), is a CX_1X_2C Cu(I) binding site.[11,12] All of the Cu(I) proteins work in conjunction to maintain balance inside the cell, and although most proteins that participate in each pathway have been elucidated, the mechanisms in which the copper ions are transferred from one protein binding site to the next have not been definitively determined. Since the Atox1 chaperone has been fully characterized[13,23] and most of the MBDs of ATP7A[14−19] and ATP7B[20,21] have also been determined, this copper pathway is among the most extensively studied.

The first mechanism for Cu(I) transfer between two CX_1X_2C binding sites was proposed by O'Halloran and co-workers in 1997.[22] The mechanism included both two- and three-coordinate Cu-bridged intermediates between the yeast chaperone, Atx1, and the acceptor protein, *Ccc*2 (homologues of the human Atox1 chaperone and the ATP7A or ATP7B acceptor proteins). Cu(I) was proposed to initially bind to the N-terminal Cys on the *Ccc*2 binding site and form a three-coordinate species, then form a two-coordinate intermediate by the breaking the S−Cu bond of Cys15 on Atx1, followed by a second three-coordinate intermediate by forming a Cu−S bond with the *Ccc*2 C-terminal Cys, and concluding with the copper only bound by the two Cys on the *Ccc*2 binding site Scheme 2. The validity of this mechanism was supported by experimental NMR structures of the two-coordinate holo-Atox1 geometry[13] and a crystal structure of an Atox1−Cu(I) dimer,[23] which has a three-coordinate Cu(I) environment. The influencing factors of this mechanism were then studied to understand the nuances of this Cu(I) transfer. In 2006, Banci et al. reported that Cu(I) is necessary for the formation of the Atx1−*Ccc*2 adduct, and without the transition-metal no interaction is formed between the donor and the acceptor proteins.[24] The environmental pH[25] along with various interface residues[26] were also experimentally observed to affect the Cu(I) transfer between Atox1 and the ATPase MBDs. Computational chemistry was recently applied to this system to investigate the details of this Cu(I) transfer further. In 2007, the delivery of Cu(I) from Atox1 to the fourth MBD of the ATP7A protein was computationally probed with quantum mechanics/molecular mechanics (QM/MM) calculations. It was predicted from this study that a four-coordinate, tetrahedral intermediate is energetically unfavorable, and two- and three-coordinate species were more likely to play a role in the transfer between binding sites.[27] Another QM/MM study was published in 2010 which argued that four- and two-coordinate intermediates are too high in energy to occur along the transfer pathway, so a transfer incorporating only three-coordinate species was proposed,[28] perhaps through an interchange mechanism. Although the relative energies in these studies gave insight into the stabilities of alternative geometries for the intermediates along plausible transfer pathways, a definitive pathway was not predicted. In this work, the electronic structure of the Cu(I) thiolate interaction is investigated to analyze the stability of two-, three-, and four-coordinate Cu(I)−Cys intermediates and to determine the potential influence it has on the Cu(I) transfer mechanism.

Scheme 2. Proposed Mechanism[22] for the Transfer of Cu(I) from the Atx1 Binding Site to the Ccc2 Binding Site via Two-Coordinate and Three-Coordinate Intermediates[a]

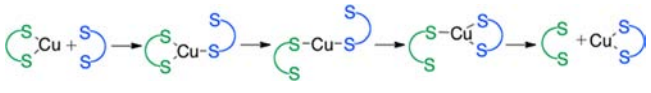

[a]The Atx1 protein is shown in green, and the Ccc2 acceptor protein is shown in blue.

The first part of this paper is dedicated to exploring the electronic structure and the bonding of three Cu(I) methylthiolate model species, $[Cu(SCH_3)_2]^{-1}$, $[Cu(SCH_3)_3]^{-2}$, $[Cu(SCH_3)_4]^{-3}$, with density functional theory (DFT). These models were studied to determine the most stable coordinations and geometries for Cu(I)-thiolate species. The second part focuses on a calculated transfer mechanism of Cu(I) from an Atox1 binding site model to a MBD of the ATP7A or ATP7B protein modeled by the dithiotreitol (DTT) ligand to determine if the electronic structure influences the transfer pathway.

COMPUTATIONAL DETAILS

All theoretical calculations were performed with the Gaussian09 suite of programs[29] and the B3LYP[30] functional. The basis set for the two-coordinate and three-coordinate Cu(I) methylthiolate models, $[Cu(SCH_3)_2]^{-1}$, $[Cu(SCH_3)_3]^{-2}$, was the Pople-type 6-31G*[31,32] basis set for all C, H, N, and O atoms and the 6-311G*[33,34] basis set for all S atoms. The Stuttgart fully relativistic 10-electron effective core potential and double-ζ basis set were used for Cu.[35] For the four-coordinate model, $[Cu(SCH_3)_4]^{-3}$, four basis sets were used because the convergence of a tetrahedral four-coordinate species could not be consistently achieved. Basis set 1 (BS1) was the same basis set as the other two-coordinate and three-coordinate models; BS2 used 6-311++G**[33,34,36] for C, H, and S atoms and cc-PVDZ[37] for the Cu, BS3 used 6-311++g** for C, H, and S atoms and cc-PVTZ[37] for the Cu, and BS4 used 6-311++g** on C, H, and S atoms and cc-PVQZ[37] for the Cu. Since the models are anionic, they were optimized in solution with the polarizable continuum model (PCM),[38] the radii and nonelectrostatic terms for Truhlar and co-workers' SMD solvation model,[39] and the solvation parameters corresponding to water to prevent an inaccurate delocalization of the negative charge toward the formation of a Rydberg-like state which can occur in gas-phase optimizations of anions.

The starting geometry for the Atox1 model was obtained from the protein data bank entry for 1TL4[13] and 1FEE,[23] since 1TL4 is a published NMR structure with 30 separate geometries reported for

dx.doi.org/10.1021/ic401106z | Inorg. Chem. 2013, 52, 10387−10393

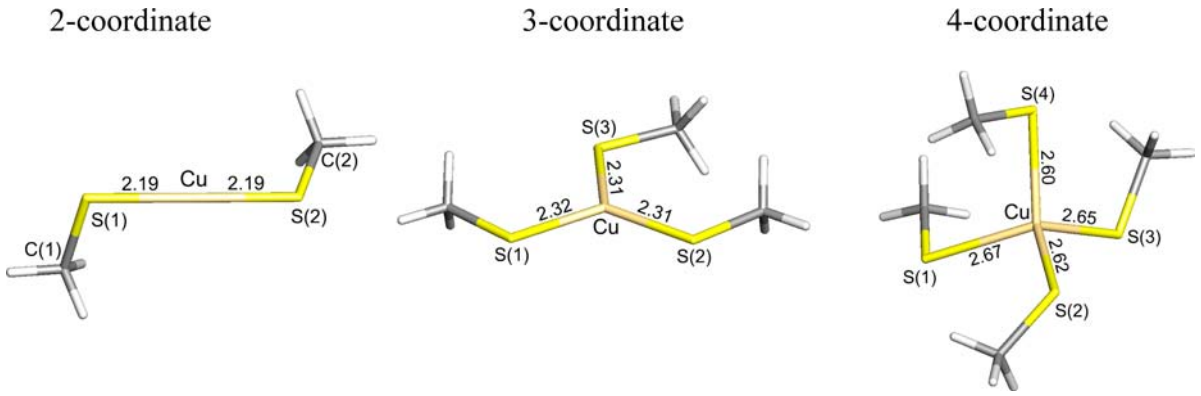

Figure 1. The calculated minimum energy geometries for the Cu(I) methylthiolate model complexes. The two-coordinate model is most stable in a linear geometry with a C−S−S−C dihedral angle of 80.3°. The trigonal planar, three-coordinate species has elongated Cu−S bonds compared to the two-coordinate model, and the C−S−S−C dihedral angles are ∼0°. The four-coordinate complex is not a stable species and could not be consistently converged.

this one entry. To ensure a precise minimum energy geometry for the model, five geometries were extracted from the database and optimized. The Atox1 dimer crystal structure, 1FEE,[23] was also optimized to ensure accuracy of the model geometry. The dimer was separated into its two Atox1 components, and then the two pieces were individually optimized with Cu(I). Initial geometries were optimized both in the gas-phase and in solution. The species calculated in the gas phase are not reported in this work because the protein backbone structure in the model was not accurately maintained in the gas-phase optimizations. However, when the solvent was included in the optimization calculations, the protein backbone in the model maintained a more accurate geometry, and therefore these structures are reported herein. The critical points in the transfer mechanism were also calculated in solution to ensure accuracy with the model species and to prevent delocalization of the negative charge. Analytical frequency calculations were performed on all final structures to ensure that either a minimum or first-order saddle point (transition state) was achieved. The 3D molecular structures displayed in this article were drawn by using the JIMP2 molecular visualization and manipulation program.[40]

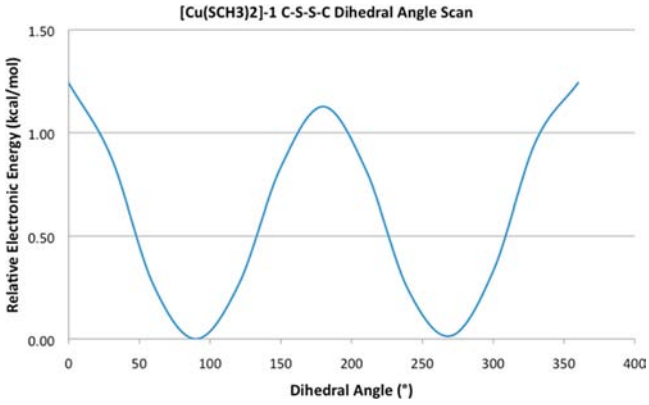

Figure 2. The potential energy for the scan of the C−S−S−C dihedral angle of $[Cu(SCH_3)_2]^{-1}$. The most stable angles are 90° and 270° when the methyl groups are perpendicular, and the least stable angles are 0° and 180° where the methyl groups are either eclipsed or anti.

RESULTS AND DISCUSSION

$[Cu(I)(SCH_3)_2]^{-1}$. The two-coordinate Cu(I) methylthiolate species was used to investigate the electronic structure of the anionic complex that forms in the CX_1X_2C binding site. The Cu(I) dimethylthiolate model converged to a near linear geometry about the Cu center with a S−Cu−S angle of 177.2° and a C−S−S−C dihedral angle of 80.3°, which are similar to the averaged experimental NMR Atox1 S−Cu−S angle of 156.4° and the C−S−S−C dihedral of 64.5°,[13] Figure 1. To examine the π interaction between the S 3p and the Cu 3d orbitals, a 360° scan was performed on the S−C−C−S dihedral angle. The scan calculated an energy potential with the lowest energy geometries having a 90° or 270 °C−S−S−C dihedral angle and the highest energy confirmations having a 180° or 0 °C−S−S−C dihedral angle, Figure 2. The potential energy for the geometry change is dominated by the interactions of the lone pair (LP) S 3p orbitals that are perpendicular to the C−S−Cu plane with the corresponding Cu 3d orbitals. To confirm that the LP-3d interaction is dictating the geometry of $[Cu(SCH_3)_2]^{-1}$, the electronic energy difference, ΔE, was calculated for the 180° and 90° geometries as a neutral singlet without the Cu atom. At a S−S bond distance of 4.38 Å, the optimized S−S distance for the $[Cu(SCH_3)_2]^{-1}$ model, the ΔE is 0.05 kcal/mol, in favor of the 90° geometry. For the $[Cu(SCH_3)_2]^{-1}$ species, the perpendicular geometry is 1.24 kcal/mol more stable than the planar geometry, so the perpendicular geometry, although favored by the S−S interaction is mainly influenced by the LP-3d interaction. As shown in Figure 3, in the planar (0° or 180°) structure the S LPs form symmetric and antisymmetric combinations, where the latter interacts strongly with one of the filled Cu 3d π orbitals. On the other hand, in the perpendicular (90° or 270°) geometries the S LPs interact with two Cu 3d π orbitals, each S LP destabilizing one Cu 3d orbital. These interactions are destabilizing because they consist of four-electron orbital−orbital repulsions; i.e., the antibonding combination is destabilized more than the bonding combination is stabilized, leading to net destabilization. In this electron-rich structure, stability is gained by adopting a geometry that distributes this LP-3d orbital (Pauli) repulsion across a maximum number of orbitals. Although distribution destabilizes a greater number of 3d orbitals, the energy increment in which they are destabilized decreases, which leads to a more stable structure overall. The preferred ∼90° dihedral angle, as seen in the NMR and crystal structures of the apo-Atox1, was an important factor in calculating the transfer mechanism.

$[Cu(I)(SCH_3)_3]^{2-}$. The three-coordinate methylthiolate complex was optimized as a doubly anionic, singlet species. The coordination around the Cu center converged to a trigonal planar geometry with the methyl groups in the same plane as

dx.doi.org/10.1021/ic401106z | Inorg. Chem. 2013, 52, 10387−10393

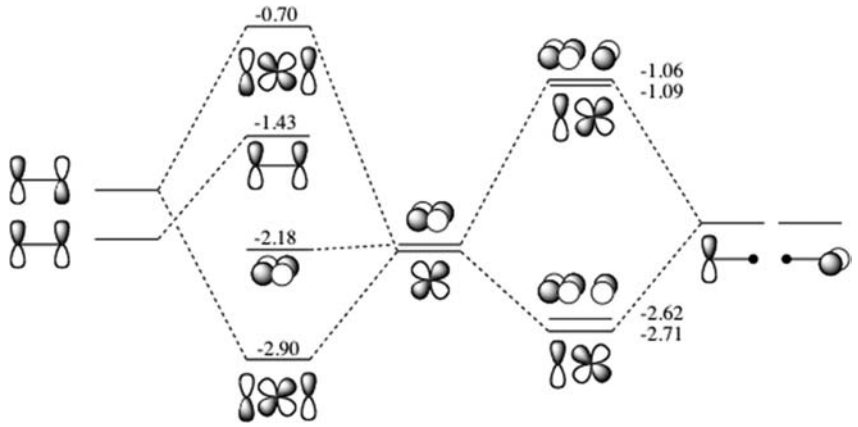

Figure 3. Molecular orbital diagrams for the two-coordinate methylthiolate copper complexes. The two copper d orbitals mix with the sulfur p orbitals differently depending on the C−S−S−C dihedral angle. With a 180° dihedral angle (left), the S p orbitals form linear combinations such that only one combination interacts repulsively with one Cu 3d orbital, while with a 90° dihedral angle (right) the S p orbitals each interact with one Cu d orbitals forming nearly degenerate pairs of bonding and antibonding orbitals. This latter situation is the more stable one.

the Cu and S atoms, Figure 1. Although the placement of the methyl groups appears quite different, the electronic origin of the geometry in the two-coordinate and three-coordinate models is determined by the same concept. Having all of the atoms in the same plane positions the S LPs perpendicular to the C−S−Cu plane where they form repulsive π interactions with the occupied Cu $3d_{xz}$ and $3d_{yx}$ orbitals, while the S 3p orbitals in the C−S−Cu plane form repulsive σ interactions with the occupied Cu $3d_{xy}$ and $3d_{x^2-y^2}$ orbitals. The alternative to this geometry would be one in which one or more of the methyl groups are rotated out of the S−Cu plane. If a methyl group is rotated to produce a C−S−Cu−S angle of 90°, the S LP would be in the same plane and repelling the same Cu 3d orbitals as the S−Cu σ repulsions. Thus, this 90° structure is higher in energy than the planar structure because the two Cu 3d orbitals in the plane are now being repelled by a larger number of interactions.

$[Cu(I)(SCH_3)_4]^{3-}$. The four-coordinate geometry around Cu(I) has been the most controversial coordination for these systems. Cu(I) forms tetrahedral complexes with donor ligands with low-lying π antibonding orbitals that can accept electron density such as CN^- or CH_3CN; however with soft, two-electron donating ligands such as sulfur or phosphorus derivatives, Cu(I) favors a two- or three-coordinate geometry. Zn(II), another d^{10} metal, readily forms tetrahedral geometries with the latter ligands, but these geometries are stable because the Zn(II) 3d orbitals are smaller in size than the Cu(I) 3d orbitals, and therefore the repulsions between the filled 3d orbitals and filled ligand orbitals are minimized.[41] NMR structures have reported linear, trigonal planar, and tetrahedral bonding schemes between Cu(I) and Atox1, but the tetrahedral geometry is always distorted with an elongated fourth Cu−S bond.[13,23] The four-coordinate, tetrahedral model was examined to determine the plausibility of a four-coordinate intermediate in the transfer mechanism. Four different basis sets were used, and during the geometry optimization with BS1, BS2, and BS4, two of the methylthiolate ligands broke their Cu−S bonds and rearranged to form interactions with the methyl hydrogens of the two methylthiolate ligands that remain bound. Upon convergence, the species adopted the near linear, two-coordinate geometry with two unbound ligands. BS3, however, seemed to have the appropriate balance of basis functions to converge a tetrahedral geometry with an average Cu−S bond length of 2.64 Å, Figure 1. The convergence with BS3 is most likely an artifact of the specific basis set because with BS4, which has a larger Cu basis set and the same S, C, H basis sets, the tetrahedral geometry does not converge. The failure to consistently optimize a tetrahedral structure lends further support to the previous conclusions that the transfer mechanism does not have a four-coordinate intermediate.

Transfer Mechanism. The binding site of the Atox1 chaperone contains the four residues Cys12-Gly13-Gly14-Cys15, so to create a model of this section the full protein was terminated before Cys12 and after Cys15. To retain more of the protein backbone structure, the Cys residues were not truncated at the α-carbon, but were extended a few atoms beyond, as shown below in a skeletal rendering of the model.

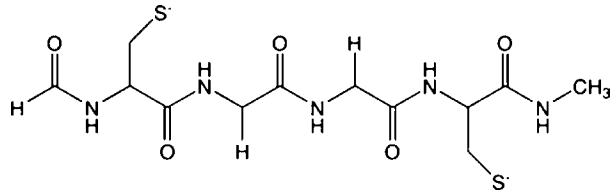

For Cys12, the NH group was included, and to maintain the sp^2 hybridization of the nitrogen a CHO group was also included in the model. Since Cys15 is more imbedded in the protein matrix than Cys12, this end of the model was extended further to include the CO group from the Cys15 residue, the NH group from the 16th residue, and was terminated with a methyl. The apoprotein was optimized as a protonated neutral species, a singly deprotonated anionic species, and a fully deprotonated dianion, while the holoprotein was optimized as a deprotonated anionic complex. All four of the converged model geometries show good agreement with the experimental structures when optimized in solution (see Supporting Information). The X_1 and X_2 residues in the MBDs of the ATP7A and ATP7B proteins are not as computationally simple as the Atox1 glycine residues, so an abbreviated model of the acceptor site was used that would be computationally efficient and differ from the Atox1 binding site model. The DTT ligand was chosen because its geometry is similar to the CX_1X_2C binding site and its small size allows for DFT calculations to be performed without large computational cost. Also, the S atoms have near free rotation, which is important for analyzing the electronic strucutre of the transfer mechanism since different

dx.doi.org/10.1021/ic401106z | Inorg. Chem. 2013, 52, 10387−10393

C−S−S−C dihedral angles were shown to stabilize the two-coordinate and three-coordinate Cu(I) methylthiolate species. The two chiral carbons on the DTT ligand can have either R,R or R,S chirality, and, although the R,S symmetry is the more stable geometry, the R,R symmetry was used because it mimics the geometry of the acceptor's binding site better than the R,S, Figure 4.

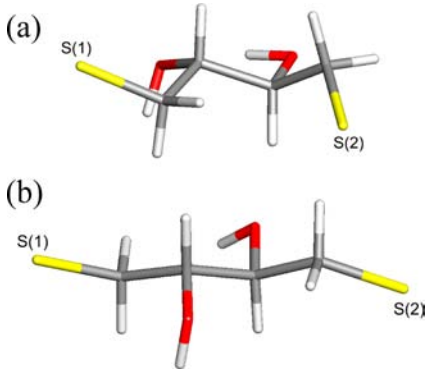

Figure 4. The optimized geometries for the doubly anionic diasteromers (a) R,R and (b) R,S confirmations of the DTT ligand. The R,S confirmation has a lower relative energy, but the R,R confirmation was used for the acceptor protein's binding site model in the transfer mechanism because the geometry is more representative of the real acceptor's binding site.

The transfer mechanism, Figure 5, begins with the two separated reactants, Cu(I) bound to the Atox1 model and the free anionic DTT ligand, which are placed at zero relative energy for the transfer mechanism. The first intermediate is the three-coordinate species, **1**, where the Cu is bound to Cys12 and Cys15 on the Atox1 model, S(1) and S(2), respectively, and one deprotonated S from the DTT ligand, S(3). Complex **1** was optimized every 60° of the 360 °C−S(3)−Cu−S(2) dihedral rotation, since the DTT ligand has free rotation about the Cu−S(3) bond. Two stable confirmations were converged from this scan, each having a C−S(3)−Cu−S(2) dihedral angle of ∼0° (see Supporting Information). The dihedral angles in these two confirmations are similar to the dihedrals calculated for the three-coordinate Cu(I) methylthiolate. In addition to the rotation about the Cu−S(3) bond, the DTT ligand can also rotate about the S(3)−C bond in this species, and when scans were run about the S(3)−C bond for the two intermediates, four more geometries were converged. The free energy differences separating the six converged species are less than 1 kcal/mol, so the orientation of the DTT ligand that most closely represented the acceptor's metal binding domain was chosen. Intermediate **1** has a trigonal planar geometry around the Cu center and an average S−Cu bond length of 2.32 Å. The DTT ligand binds with Cu so that Cu−S(3)−C are planar, but the C−S(1)−S(2)−C dihedral angle is 71.4° so neither of the methyl groups on the Atox1 model are in the same plane as the Cu−S(3)−C. The C−S(1)−S(2)−C dihedral angle is nearly identical to the 72.0 °C−S−S−C dihedral angle in the two-coordinate Atox1 model, which is believed to be a result of the rigidity of the Atox1 model's backbone. From the analysis of the $[Cu(I)(SCH_3)_3]^{-2}$ model, we would assume that this intermediate would be more stable if all three of the C−S−S−C

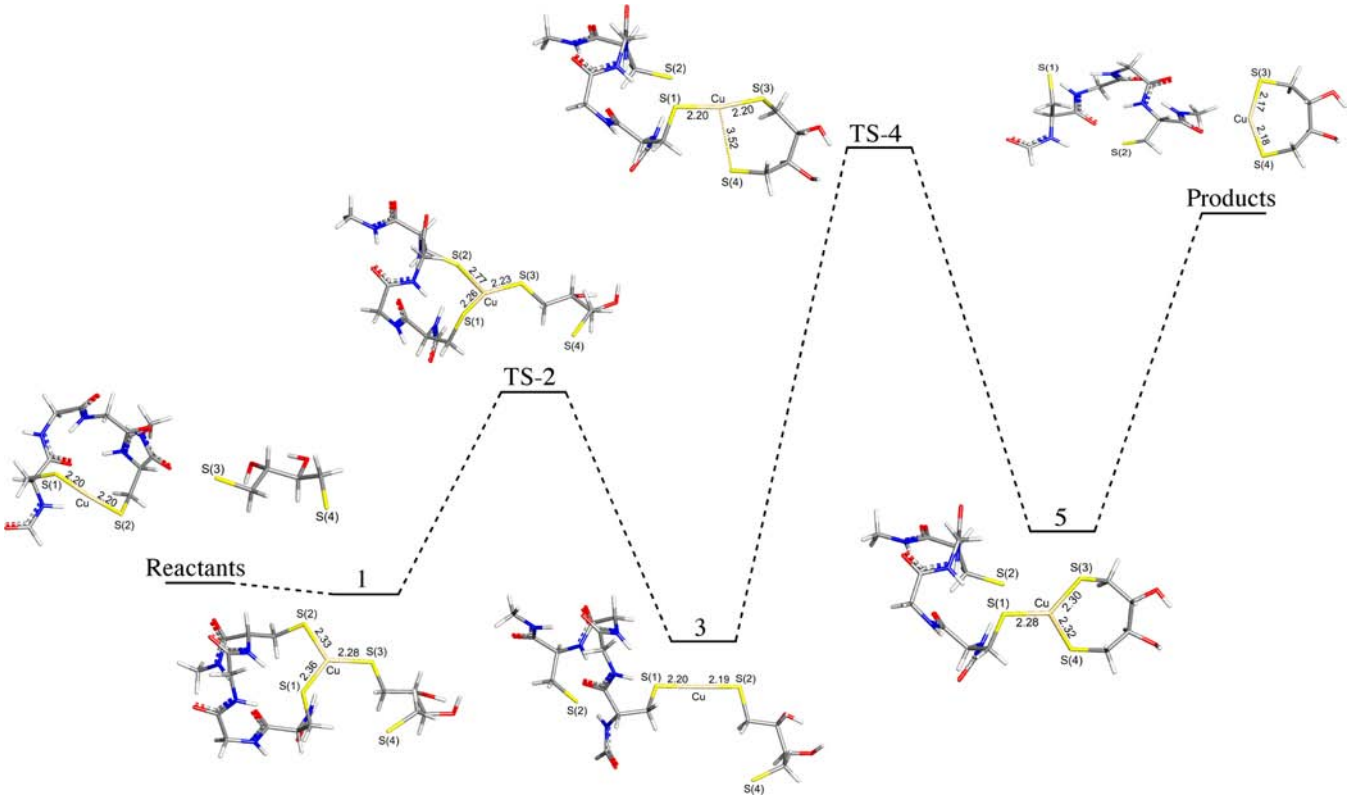

Figure 5. Enthalpy surface for the transfer of Cu(I) from the Atox1 binding site model to the DTT ligand. The transfer begins with the Cu-bound Atox1 binding to S(3) from the DTT ligand (**1**). Dissociation of the Cu−S(2) bond (**TS-2**) forms a two-coordinate intermediate (**3**), and then S(4) binds to form **5**. Finally, S(1) breaks releasing Atox1 and Cu is bound solely by DTT.

dx.doi.org/10.1021/ic401106z | *Inorg. Chem.* 2013, 52, 10387−10393

dihedral angles were ∼0°; however, maintaining a less stable geometry for this intermediate might be related to the lower energy transition state and possibly a faster transfer.

The first transition state in the mechanism, **TS-2**, involves cleaving the S(2)−Cu bond on the Atox1 model. The S(2)−Cu bond was broken first instead of the S(1)−Cu bond because Cys15 is located more deeply inside the protein matrix than the largely solvent exposed Cys12, and the Cu−Cys15 bond has been experimentally predicted to break first.[23] Most of the rearrangement in the transition state is concentrated around the S(2) and Cu atoms as their bond is cleaved, but, as this is occurring, the S(1)−Cu−S(3) angle is also expanding to the two-coordinate, linear geometry. The relative enthalpy barrier for **TS-2** is low, 2.99 kcal/mol, which leads one to assume that the breaking of the S(2)−Cu bond occurs quickly. Intermediate **3** is the lowest energy species in the transfer mechanism, and it is the only intermediate with a two-coordinate geometry, aside from the reactants and products. The Cu−S bond lengths have decreased from an average of 2.32 Å in **1** to 2.19 Å, the S(1)−Cu−S(3) angle has increased to 176.7°, and the C−S(1)−S(3)−C dihedral angle has increased to 78.5°. The bonding at the Cu center is very similar to the bonding in the $[Cu(I)(SCH_3)_2]^{-1}$ complex, where the LPs on the two S atoms form a repulsive π interaction with two Cu 3d orbitals instead of only one.

In step four of the transfer, **TS-4**, the second, three-coordinate complex is formed as S(4) transitions to bond with the Cu. In this transition state, the CH_2 group bound to S(3) has to rotate 180° to allow S(4) to bind to the Cu. Without the rotation of the $-CH_2$ group, **TS-4** could not be calculated because the resultant three-coordinate intermediate is not stable. The rotation of the $-CH_2$ group allows for the adoption of a more stable LP-3d orientation in intermediate **5** which follows the transition state. **TS-4** has a relative enthalpy of 6.14 kcal/mol compared to **1** in the mechanism. For the final intermediate of the mechanism, the Cu−S bond distances are elongated back to an average of 2.30 Å, while the three-coordinate, trigonal planar geometry is assumed. The binding scheme in **5** is similar to that of **1** with the roles of the two binding sites reversed. The Atox1 model now has free rotation because it is only bound by S(1), so it assumes a C−S(1)−Cu−S(4) dihedral angle of 3.6°, which would allow for the ideal interaction between the S LP and Cu 3d orbitals. Although the Cu−S binding and orientation is the same in **1** and **5**, the DTT ligand experiences more ring strain overall compared to the Atox1 model, so the relative free energy for **5** is higher than **1**.

The final products are higher in energy than the reactants, but for the actual transfer between Atox1 and an ATP7A or ATP7B MBD this is not the case because the binding sites on these proteins have been experimentally determined to have a higher affinity for Cu(I) than Atox1. An intermediate such as **5** in a transfer mechanism where the acceptor is a model of a MBD and not DTT could have a lower energy than the reactants, a result that would mimic the experimental binding affinities. On the other hand, the instability of **5** might encourage breaking the Cu−S(1) bond faster since the two-coordinate product is more stable.

CONCLUSION

The electron-rich Cu(I) thiolate interaction was computationally investigated to evaluate the stability of various Cu(I)−Cys coordination environments and to predict if the transition-metal's electronic structure influences the transfer pathway. The $[Cu(SCH_3)_2]^{-1}$ model showed maximum stability with a C−S−S−C dihedral angle of 90°, which was also observed in the Atox1 and DTT two-coordinate complexes. The trigonal planar, three-coordinate complex's stability is maximized by maintaining a more planar geometry around the Cu center, which distributes the LP-3d orbital repulsions across the maximum number of interactions. A four-coordinate, tetrahedral model of $[Cu(SCH_3)_4]^{-3}$ could not be consistently converged, and from the molecular orbital diagram of the complex, a four-coordinate geometry is not likely to be stable. These conclusions were utilized to calculate a mechanism which encompassed five steps that include three-coordinate and two-coordinate stationary points that resemble the previously reported transfer intermediates connected by low energy transition states. A mechanism where the initial step is dissociative was concluded to be unlikely because a one-coordinate species is ∼30 kcal/mol higher in energy than the initial associative three-coordinate intermediate. A fully associative mechanism was also predicted to be improbable because a four-coordinate intermediate along the reaction path failed to successfully converge. The structural agreement that the model system geometries have with experimentally observed intermediates supports the conclusion that the electronic structure and bonding between Cu(I) and the Cys residues influence the transfer mechanism. The Cu(I)−Cys electronic structure has influence in concert with the van der Waals and electrostatic interactions that occur among the interface residues and the variation of the conformational space to determine the configuration of the donor−acceptor adduct.

Table 1. Electronic Energies, Enthalpies, and Free Energies for the Calculated Transfer Mechanism

	ΔE	ΔH	ΔG
reactants	0.00	0.00	0.00
1	−0.99	−0.21	11.51
TS-2	2.72	2.99	14.44
3	−1.93	−0.99	9.54
TS-4	5.81	6.14	18.88
5	−0.58	0.40	12.90
products	6.04	5.31	2.76

ASSOCIATED CONTENT

Supporting Information

Figure S1: Calculated geometries for the CGGC residue fragment from the Atox1 binding site. Figure S2: Optimized confirmations of intermediate 1 due to the rotation of the DTT about the Cu−S(3) bond and the S(3)−C bond. This material is available free of charge via the Internet at http://pubs.acs.org.

AUTHOR INFORMATION

Corresponding Author

*E-mail: mbhall@tamu.edu.

Notes

The authors declare no competing financial interest.

ACKNOWLEDGMENTS

This work was supported by the National Science Foundation under Grant CHE0910552 and The Welch Foundation under grant A-0648.

REFERENCES

(1) Tümer, Z.; Møller, L. B. *Eur. J. Hum. Genet.* **2010**, *18*, 511−518.

(2) Cuillel, M. *J. Incl. Phenom. Macrocycl. Chem.* **2009**, *65*, 165.
(3) Rosen, D. R.; Siddique, T.; Patterson, D.; Figlewicz, D. A.; Sapp, P.; Hentati, A.; Donaldson, D.; Goto, J.; O'Regan, J. P.; Deng, H.-X.; Rahmani, Z.; Krizus, A.; Mckenna-Yasek, D.; Cayabyab, A.; Gaston, S. M.; Berger, R.; Tanzi, R. E.; Halperin, J. J.; Herzfeldt, B.; Van den Bergh, R.; Hung, W.-Y.; Bird, T.; Deng, G.; Mulder, D. W.; Smyth, C.; Laing, N. G.; Soriano, E.; Pericak-Vance, M. A.; Haines, J.; Rouleau, G. A.; Gusella, J. S.; Horvitz, H. R.; Brown, R. H., Jr. *Nature* **1993**, *362*, 59.
(4) Das, K. S.; Ray, K. *Nat. Clin. Pract. Neurol.* **2006**, *2*, 482.
(5) Huang, X. D.; Cuajungco, M. P.; Atwood, C. S.; Hartshorn, M. A.; Tyndall, J. D. A.; Hanson, G. R.; Stokes, K. C.; Leopold, M.; Multhaup, G.; Goldstein, L. E.; Scarpa, R. C.; Saunders, A. J.; Lim, J.; Moir, R. D.; Glabe, C.; Bowden, E. F.; Masters, C. L.; Fairlie, D. P.; Tanzi, R. E.; Bush, A. I. J. *Biol. Chem.* **1999**, *274*, 37111.
(6) Viles, J. H.; Cohen, F. E.; Prusiner, S. B.; Goodin, D. B.; Wright, P. E.; Dyson, H. J. *Proc. Natl. Acad. Sci. U. S. A.* **1999**, *96*, 2042.
(7) Banci, L.; Bertini, I.; McGreevy, K. S.; Rosato, A. *Nat. Prod. Rep.* **2010**, *27*, 695.
(8) Kim, B. E.; Nevitt, T.; Thiele, D. J. *Nat. Chem. Biol.* **2008**, *4*, 176.
(9) Robinson, N. J.; Winge, D. R. *Annu. Rev. Biochem.* **2010**, *79*, 537.
(10) O'Halloran, T. V.; Culotta, V. C. *J. Biol. Chem.* **2000**, *275*, 25057.
(11) (a) Banci, L.; Bertini, I.; Cantini, F.; Della-Malva, N.; Migliardi, M.; Rosato, A. *J. Biol. Chem.* **2007**, *282*, 23140. (b) Banci, L.; Bertini, I.; Cantini, F.; Massagni, C.; Migliardi, M.; Rosato, A. *J. Biol. Chem.* **2009**, *284*, 9354.
(12) Keller, A. M.; Benítez, J. J.; Klarin, D.; Zhong, L.; Goldfogel, M.; Yang, F.; Chen, T.-Y.; Chen, P. *J. Am. Chem. Soc.* **2012**, *134*, 8934.
(13) Anastassopoulou, I.; Banci, L.; Bertini, I.; Cantini, F.; Katsari, E.; Rosato, A. *Biochem.* **2004**, *43*, 13046.
(14) Gitschier, J.; Moffat, B.; Reilly, D.; Wood, W. I.; Fairbrother, W. J. *Nat. Struct. Biol.* **1998**, *5*, 47.
(15) Banci, L.; Bertini, I.; Del Conte, R.; D'Onofrio, M.; Rosato, A. *Biochemistry* **2004**, *43*, 3396.
(16) Banci, L.; Bertini, I.; Cantini, F.; Chasapis, C. T.; Hadjiliadis, N.; Rosato, A. *J. Biol. Chem.* **2005**, *280*, 38259.
(17) Banci, L.; Bertini, I.; Cantini, F.; Migliardi, M.; Rosato, A.; Wang, S. *J. Mol. Biol.* **2005**, *352*, 409.
(18) DeSilva, T. M.; Veglia, G.; Opella, S. J. *Proteins* **2005**, *61*, 1038.
(19) Banci, L.; Bertini, I.; Cantini, F.; DellaMalva, N.; Herrmann, T.; Rosato, A.; Wüthrich, K. *J. Biol. Chem.* **2006**, *281*, 29141.
(20) Banci, L.; Bertini, I.; Cantini, F.; Rosenzweig, A. C.; Yatsunyk, L. A. *Biochemistry* **2008**, *47*, 7423.
(21) Achila, D.; Banci, L.; Bertini, I.; Bunce, J.; Ciofi-Baffoni, S.; Huffman, D. L. *Proc. Natl. Acad. Sci. U. S. A.* **2006**, *103*, 5729.
(22) Pufahl, R. A.; Singer, C. P.; Peariso, K. L.; Lin, S.-J.; Schmidt, P. J.; Fahrni, C. J.; Culotta, V. C.; Penner-Hahn, J. E.; O'Halloran, T. V. *Science* **1997**, *278*, 853.
(23) Wernimont, A. K.; Huffman, D. L.; Lamb, A. L.; O'Halloran, T. V.; Rosenzweig, A. C. *Nat. Struct. Biol.* **2000**, *7*, 766.
(24) Banci, L.; Bertini, I.; Cantini, F.; Felli, I. C.; Gonnelli, L.; Hadjiliadis, N.; Pierattelli, R.; Rosato, A.; Voulgaris, P. *Nat. Chem. Biol.* **2006**, *2*, 367.
(25) Badarau, A.; Dennison, C. *J. Am. Chem. Soc.* **2011**, *133*, 2983.
(26) (a) Banci, L.; Bertini, I.; Calderone, V.; Della-Malva, N.; Felli, I. C.; Neri, S.; Pavelkova, A.; Rosato, A. *Biochem. J.* **2009**, *422*, 37. (b) Hussain, F.; Rodriguez-Granillo, A.; Wittung-Stafshede, P. *J. Am. Chem. Soc.* **2009**, *131*, 16371.
(27) Holt, B. T. O.; Merz, K. M., Jr. *Biochem.* **2007**, *46*, 8816.
(28) Rodriguez-Granillo, A.; Crespo, A.; Estrin, D. A.; Wittung-Stafshede, P. *J. Phys. Chem. B* **2010**, *114*, 3698.
(29) Frisch, M. J.; Trucks, G. W.; Schlegel, H. B.; Scuseria, G. E.; Robb, M. A.; Cheeseman, J. R.; Scalmani, G.; Barone, V.; Mennucci, B.; Petersson, G. A.; Nakatsuji, H.; Caricato, M.; Li, X.; Hratchian, H. P.; Izmaylov, A. F.; Bloino, J.; Zheng, G.; Sonnenberg, J. L.; Hada, M.; Ehara, M.; Toyota, K.; Fukuda, R.; Hasegawa, J.; Ishida, M.; Nakajima, T.; Honda, Y.; Kitao, O.; Nakai, H.; Veven, T.; Montgomery, J. A.; , Jr., Peralta, J. E.; Ogliaro, F.; Bearpark, M.; Heyd, J. J.; Brothers, E.; Kudin, K. N.; Staroverov, V. N.; Kobayashi, R.; Normand, J.; Raghavachari, K.; Rendell, A.; Burant, J. C.; Iyengar, S. S.; Tomasi, J.; Cossi, M.; Rega, N.; Millam, J. M.; Klene, M.; Knox, J. E.; Cross, J. B.; Bakken, V.; Adamo, C.; Jaramillo, J.; Gomperts, R.; Stratmann, R. E.; Yazyev, O.; Austin, A. J.; Cammi, R.; Pomelli, C.; Ochterski, J. W.; Martin, R. L.; Morokuma, K.; Zakrzewski, V. G.; Voth, G. A.; Salvador, P.; Dannenberg, J. J.; Dapprich, S.; Daniels, A. D.; Farkas, O.; Foresman, J. B.; Ortiz, J. V.; Cioslowski, J.; and Fox, D. J. *Gaussian 09*, Revision A.02; Gaussian, Inc.: Wallingford, CT, 2009.
(30) (a) Becke, A. D. *J. Chem. Phys.* **1993**, *98*, 5648. (b) Stephens, P. J.; Devlin, F. J.; Chabalowski, C. F.; Frisch, M. J. *J. Phys. Chem.* **1994**, *98*, 11623. (c) Lee, C. T.; Yang, W. T.; Parr, R. G. *Phys. Rev. B* **1988**, *37*, 785−789.
(31) Hariharan, P. C.; Pople, J. A. *Theoret. Chim. Acta* **1973**, *28*, 213 (diffuse).
(32) (a) Petersson, G. A.; Al-Laham, M. A. *J. Chem. Phys.* **1991**, *94*, 6081. (b) Petersson, G. A.; Bennett, A.; Tensfeldt, T. G.; Al-Laham, M. A.; Shirley, W. A.; Mantzaris, J. *J. Chem. Phys.* **1988**, *89*, 2193.
(33) Krishnan, R.; Binkley, J. S.; Seeger, R.; Pople, J. A. *J. Chem. Phys.* **1980**, *72*, 650.
(34) McLean, A. D.; Chandler, G. S. *J. Chem. Phys.* **1980**, *72*, 5639.
(35) (a) Figgen, D.; Rauhut, G.; Dolg, M.; Stoll, H. *Chem. Phys.* **2005**, *311*, 227. (b) Peterson, K. A.; Puzzarini, , C. *Theor. Chem. Acc.* **2005**, *114*, 283.
(36) Clark, T.; Chandrasekhar, J.; Spitznagel, G. W.; Schleyer, P. v. R. *J. Comput. Chem.* **1983**, *4*, 294.
(37) Dunning, T. H., Jr. *J. Chem. Phys.* **1989**, *90*, 1007.
(38) Scalmani, G.; Frisch, M. J. 2009, unpublished work.
(39) Marenich, A. V.; Cramer, C. J.; Truhlar, D. G. *J. Phys. Chem. B* **2009**, *113*, 6378.
(40) (a) Manson, J.; Webster, C. E.; Hall, M. B. *JIMP2, Version 0.091, a free program for visualizing and manipulating molecules*; Texas A&M University: College Station, TX, 2006. (b) Hall, M. B.; Fenske, R. F. *Inorg. Chem.* **1972**, *11*, 768.
(41) CottonF. A.WilkinsonG. *Advanced Inorganic Chemistry* , 5th ed.; Wiley: New York, 1988; p 755.